Synchronizations in Oscillatory Networks with Memristor Couplings as Ring Structure

Yukinojo Kotani, Yoko Uwate and Yoshifumi Nishio
Dept. Electrical and Electronic Eng.,
Tokushima University
Email: {kotani, uwate, nishio}@ee.tokushima-u.ac.jp

2024 IEEE International Symposium on Circuits and Systems (ISCAS) | 979-8-3503-3099-1/24/$31.00 ©2024 IEEE | DOI: 10.1109/ISCAS58744.2024.10558633

***Abstract*—In this study, we propose the coupled oscillatory networks with the memristor couplings as a ring structure. We focus on the dynamics of the memristor couplings, and investigate synchronization phenomena. As a result, this study observes three different synchronization state types: multi-phase synchronization state, in-phase and anti-phase synchronization state and amplitude death. In addition, we analyze the power consumption of the memristor couplings to make clear the cause of phase sift.**

I. Introduction

Synchronization phenomena observed from the coupled oscillatory networks have been studied. Many studies related to synchronization phenomena in oscillatory networks have important roles: optimizing the power operation of microgrid [1], [2], realizing associative memory for patients with prosopagnosia [3], [4] and analyzing the characteristics of networks [5]-[9]. Besides, network structures affect data communication. A ring structure has the property of preventing communication disconnected compared to other structures. Therefore, synchronization phenomena in the oscillatory networks as a ring structure need to be investigated.

A memristor is the fourth basic circuit elements; a resistor, a capacitor and an inductor. It is introduced by L. O. Chua in 1971 [10], and it was developed by Hewlett-Packard Lab in 2008 [11]. Resistance value of a memristor is characterized by a charge or a flux, whereas a resistor is characterized by a current or a voltage. The charge and the flux are defined as the integral of the current and the voltage respectively. The memristor has the dynamics compared to the resistor.

In previous studies, synchronization phenomena in the coupled oscillatory networks were investigated. The coupled oscillatory networks via resistors, time-varying resistors and fifth-power resistors were proposed [12]-[14]. Recently, various coupled circuits with the memristor couplings were proposed [15]. Therefore, this study focuses on the dynamics of the memristor couplings in the oscillatory networks.

In this study, we focus on using the memristor couplings in the oscillatory networks. We investigate synchronization state types analyzing the time-series of the voltages, the memristors and the phase differences. In addition, we also investigate the cause and effect relationship between synchronization state types and the dynamics of the memristor by calculating the power consumption of the memristor couplings.

II. Oscillatory Network Model

Figure 1 (a) shows the schematic model of the memristor. Resistance value of the memristor is memristance $M(q)$. Memristance is defined as the gradient of the charge q - flux φ characteristics curve in Fig. 1 (b).

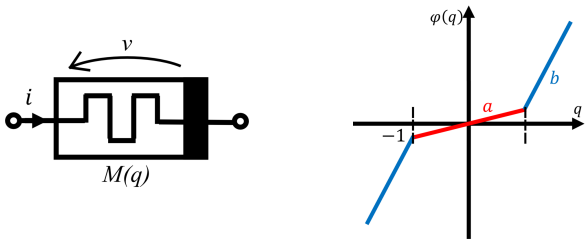

(a) (b)

Fig. 1: Memristor model. (a): Schematic model, (b): $q-\varphi$ curve.

The $q-\varphi$ is characterized by the piecewise-linear function $\varphi(q)$ as Eq. (1) [16].

$$M(q)=\frac{d\varphi(q)}{dq}=\begin{cases}a & (|q|<1)\\ b & (|q|>1)\end{cases} \qquad (1)$$
$$\varphi(q)=bq+0.5(a-b)(|q+1|-|q-1|).$$

Figure 2 shows the Nth-oscillatory network with the memristor couplings as a ring structure. r is the tiny resistors to avoid L-loop.

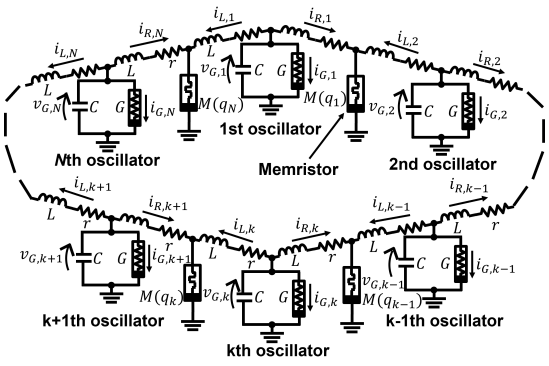

Fig. 2: Nth-oscillatory network with memristor couplings as a ring structure.

Circuit equations are obtained from Kirchhoff's laws as Eq. (2). These equations need to be normalized to investigate the synchronization states by using computer simulations.

$$\begin{cases} C\dfrac{dv_k}{dt} = -i_{Gk} - i_{R,k} - i_{L,k} \\ 2L\dfrac{di_{R,k}}{dt} = v_k - ri_{R,k} - M(q_k)(i_{R,k} + i_{L,k+1}) \\ 2L\dfrac{di_{L,k}}{dt} = v_k - ri_{L,k} - M(q_k)(i_{R,k-1} + i_{L,k}) \\ \dfrac{dq_k}{dt} = i_{R,k} + i_{L,k+1} \\ M(q_k) = \dfrac{d\varphi(q_k)}{dq_k} = \begin{cases} a & (|q_k| < 1) \\ b & (|q_k| > 1) \end{cases} \\ \varphi(q_k) = bq_k + 0.5(a-b)(|q_k+1| - |q_k-1|). \end{cases} \tag{2}$$

The variables and the parameters are defined as Eq. (3).

$$\begin{aligned} v_k = \sqrt{\frac{g_1}{g_3}}x_k, i_{R,k} = \sqrt{\frac{g_1 C}{g_3 L}}y_{R,k}, i_{L,k} = \sqrt{\frac{g_1 C}{g_3 L}}y_{L,k}, q_k = z_k, \\ t = \sqrt{LC}\tau, \varepsilon = g_1\sqrt{\frac{L}{C}}, \gamma = \sqrt{\frac{C}{L}}, \zeta = C\sqrt{\frac{g_1}{g_3}}, \eta = r\sqrt{\frac{C}{L}}. \end{aligned} \tag{3}$$

The normalized circuit equations are obtained by changing the variables and the parameters.

$$\begin{cases} \dfrac{dx_k}{d\tau} = \varepsilon(1 - x_k^2)x_k - y_{R,k} - y_{L,k} \\ \dfrac{dy_{R,k}}{d\tau} = \dfrac{1}{2}(x_k - \eta y_{R,k} - \gamma M(z_k)(y_{R,k} + y_{L,k+1})) \\ \dfrac{dy_{L,k}}{d\tau} = \dfrac{1}{2}(x_k - \eta y_{L,k} - \gamma M(z_k)(y_{R,k-1} + y_{L,k})) \\ \dfrac{dz_k}{d\tau} = \zeta(y_{R,k} + y_{L,k+1}) \\ M(z_k) = \dfrac{d\varphi(z_k)}{dz_k} = \begin{cases} a & (|z_k| < 1) \\ b & (|z_k| > 1) \end{cases} \\ \varphi(z_k) = bz_k + 0.5(a-b)(|z_k+1| - |z_k-1|). \end{cases} \tag{4}$$

Where τ is the scaling time, ε is the nonlinearity, γ is the coupling strength, ζ is the coupling factor and η is the factor of the tiny resistor.

The instantaneous power $p(t)$ of the memristor is defined as Eq. (5). $i(t)$ is the current through the memristor.

$$p(t) = M(q(t))i(t)^2. \tag{5}$$

The average power consumption is described as follows. T is a long period of the oscillator. $P_{i,j}$ means the average power consumption of the memristor between the ith-oscillator and jth-oscillator Therefore, the total of the average power consumption P_{all} in the oscillatory network with the memristor couplings can be calculated by Eq. (6).

$$\begin{aligned} P_{all} &= P_{1,2} + P_{2,3} + ... + P_{N-1,N} + P_{N,1} \\ &= \frac{1}{T}\sum_{k=1}^{N}\gamma M(z_k)(y_{R,k} + y_{L,k+1})^2. \end{aligned} \tag{6}$$

III. Results

In this study, the normalized circuit equations were calculated by the Runge-Kutta method with step size $h = 0.01$. The scaling time $\tau = 20,000$. The parameters were set to $\varepsilon = 0.1$, $\gamma = 1$, $\zeta = 0.1$ and $\eta = 0.001$. We carried out the simulations for the cases of $N = 3, 5, 7$ and 9. For the cases of $N = 3, 5$ and 7, the parameters of the memristors $a = 0.1$ and $b = 10$. For the case of $N = 9$, $a = 0.05$ and $b = 10$.

A. Synchronization Phenomena

In this section, we analyzed the time-series of x and the phase differences to research synchronization state types changing the initial values of x, y and z. The phase differences are calculated by using Poincaré maps. The methods of calculating the phase differences are described as follows.

1) The van der Pol oscillator with third-power has a stable limit cycle, so Poincaré section is defined as the plane that $x > 0$ and $y = 0$ in phase plane.
2) If x_1 and y_1 move from fourth quadrant to first quadrant ($x_1(\tau - 1) > 0$, $y_1(\tau - 1) < 0$ and $y_1(\tau) > 0$), each of the relative phase difference for first oscillator is calculated. Count is the number of the times that the solutions x_1 and y_1 move from fourth quadrant to first quadrant.

Also, we analyzed the time-series of M to investigate the cause and effect relationship between the dynamics of memristors and synchronization state types. Figure 3, 4, 5 and 6 show the simulation results. We confirmed three different synchronization state types: Nth-phase synchronization state, in-phase and anti-phase synchronization state and amplitude death.

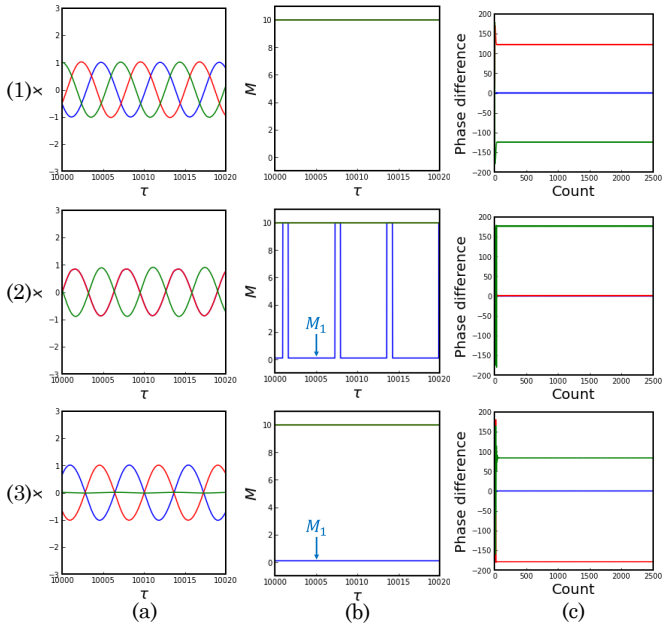

Fig. 3: Simulation results ($N = 3$). (1): Three-phase, (2): In-phase and anti-phase, (3): Amplitude death, (a): Time-series of x, (b): Time-series of M, (c): Phase differences.

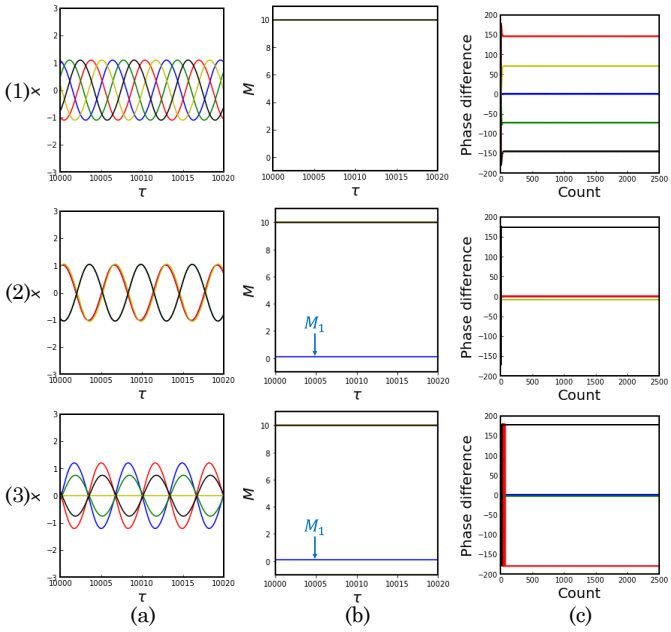

Fig. 4: Simulation results ($N = 5$). (1): Five-phase, (2): In-phase and anti-phase, (3): Amplitude death, (a): Time-series of x, (b): Time-series of M, (c): Phase differences.

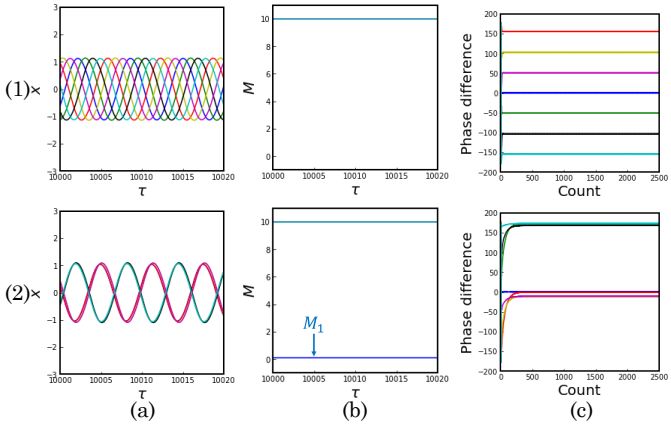

Fig. 5: Synchronization results ($N = 7$). (1): Seven-phase, (2): In-phase and anti-phase, (a): Time-series of x, (b): Time-series of M, (c): Phase differences.

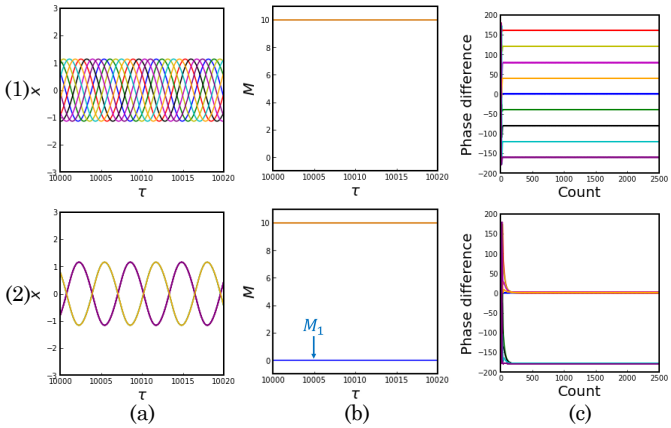

Fig. 6: Synchronization results ($N = 9$). (1): Nine-phase, (2): In-phase and anti-phase, (a): Time-series of x, (b): Time-series of M, (c): Phase differences.

In these simulation results, for the case (1), Nth-phase synchronization state were observed because all memristances assumed b constant. This tendency had already been confirmed in the Nth-oscillatory network with the resistors as a ring structure. In the cases (2) and (3), in-phase and anti-phase synchronization state and amplitude death were confirmed because M_1 assumed a and the other memristances assumed b. Therefore, in-phase and anti-phase synchronization states and amplitude death were arisen from the dynamics of the memristor couplings.

B. Power Consumption

In Sec. III A, we reported that three synchronization state types; Nth-phase synchronization, in-phase and anti-phase synchronizations and amplitude death were caused by the dynamics of the memristors. In this section, we analyzed the power consumption of the memristors to make clear the cause of that in-phase and anti-phase synchronization state and amplitude death. Figure 7, 8, 9 and 10 show the time-series of the instantaneous power of the memristors and the total instantaneous power for each synchronization type in the Nth oscillatory networks ($N = 3, 5, 7, 9$).

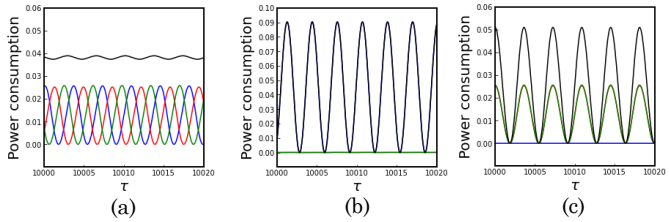

Fig. 7: Time-series of instantaneous power of memristors ($N = 3$). (a): Three-phase, (b): In-phase and anti-phase, (c): Amplitude death.

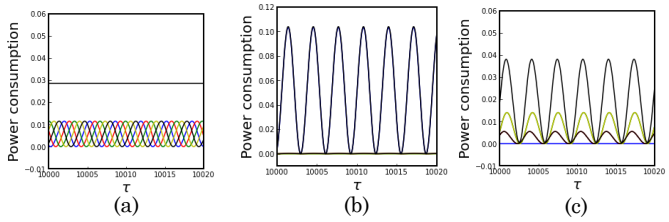

Fig. 8: Time-series of instantaneous power of memristors ($N = 5$). (a): Five-phase, (b): In-phase and anti-phase, (c): Amplitude death.

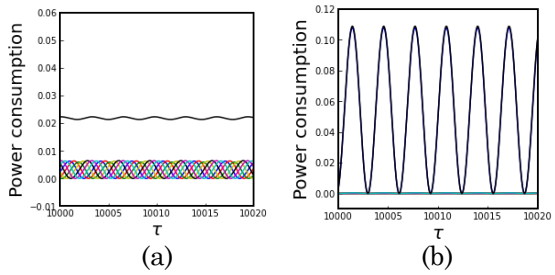

Fig. 9: Time-series of instantaneous power of memristors ($N = 7$). (a): Seven-phase, (b): In-phase and anti-phase.

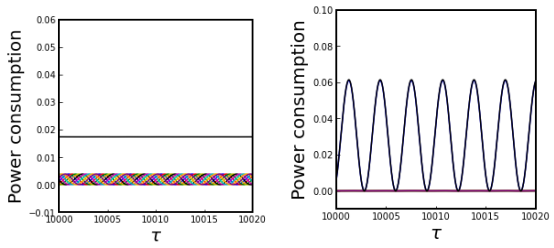

(a) (b)

Fig. 10: Time-series of instantaneous power of memristors ($N = 9$). (a): Nine-phase, (b): In-phase and anti-phase.

For the case of in-phase and anti-phase synchronizations state, even number pairs of anti-phase components were canceled each other and the other component are not canceled. The amplitude of the instantaneous power was much larger than the case of N phase synchronization. For the case of amplitude death, even number pairs of anti-phase components were canceled each other and the amplitude of the other component was dead. Therefore, the amplitude of the instantaneous power was much smaller than the case of Nth-phase synchronization.

Next, Table I, II, III and IV summarize the average power consumption compared Nth-phase synchronization, in-phase and anti-phase synchronizations and amplitude death.

TABLE I: Average Power Consumption ($N = 3$).

Power	Synchronization State types		
	Three-phase	In-phase and Anti-phase	Amplitude death
$P_{1,2}$	0.0128	0.0452	0.00000485
$P_{2,3}$	0.0125	0.0000585	0.0127
$P_{3,1}$	0.0128	0.0000574	0.0128
P_{all}	0.0382	0.0453	0.0255

TABLE II: Average Power Consumption ($N = 5$).

Power	Synchronization State Types		
	Five-phase	In-phase and Anti-phase	Amplitude death
$P_{1,2}$	0.0124	0.103	0.000117
$P_{2,3}$	0.0127	0.00155	0.00659
$P_{3,4}$	0.0129	0.0148	0.0155
$P_{4,5}$	0.0131	0.00173	0.0157
$P_{5,1}$	0.0133	0.00218	0.00540
P_{all}	0.0643	0.110	0.0434

TABLE III: Average Power Consumption ($N = 7$).

Power	Synchronization State Types	
	Seven-phase	In-phase and Anti-phase
$P_{1,2}$	0.00727	0.106
$P_{2,3}$	0.00754	0.00170
$P_{3,4}$	0.00733	0.00167
$P_{4,5}$	0.00788	0.00189
$P_{5,6}$	0.00831	0.00207
$P_{6,7}$	0.00857	0.000236
$P_{7,1}$	0.00873	0.000447
P_{all}	0.0556	0.116

TABLE IV: Average Power Consumption ($N = 9$).

Power	Synchronization State Types	
	Nine-phase	In-phase and Anti-phase
$P_{1,2}$	0.00492	0.0634
$P_{2,3}$	0.00512	0.00147
$P_{3,4}$	0.00533	0.00192
$P_{4,5}$	0.00557	0.00253
$P_{5,6}$	0.00583	0.00328
$P_{6,7}$	0.00609	0.00401
$P_{7,8}$	0.00639	0.00476
$P_{8,9}$	0.00669	0.00521
$P_{9,1}$	0.00697	0.00186
P_{all}	0.0529	0.0887

In these simulations, for the case of Nth-phase synchronization, each of the average power consumption was the almost same values because all memristances equaled to b. For the case of in-phase and anti-phase synchronizations state, even number pairs of anti-phase components were canceled each other and the other component were not canceled, so the total average power consumption was much larger than the case of Nth-phase synchronization. However, for the case of amplitude death, even number pairs of anti-phase components were also canceled each other and the amplitude of the other component was dead, so the total average power consumption of the case of amplitude death was less than the case of Nth-phase synchronization. Therefore, our simulation results show that in-phase and anti-phase synchronizations state and amplitude death in the Nth-oscillatory networks as a ring structure is caused by the dynamics of the memristor couplings.

IV. Conclusions

In this study, we have proposed the coupled oscillatory networks with the memristor couplings as a ring structure. We investigated synchronization state types by analyzing the time-series of the voltage, the memristors and the phase differences. As a result, in-phase and anti-phase synchronization and amplitude death were obtained by the dynamics of the memristors. In addition, we investigated the cause and effect relationship between the synchronization state types and the dynamics by calculating the power consumption of the memristor. For the case of in-phase and anti-phase synchronizations state, the power consumption of the memristors was larger than the case of multi-phase synchronizations. On the other hand, for the case of amplitude death, the power consumption of the memristors was smaller than the case of multi-phase synchronizations. Therefore, we confirmed that the power consumption of the memristor couplings affects the synchronization states. Also, we confirmed that synchronization states depend on the dynamics of the memristor couplings.

For the future works, we would like to use theoretical analysis and circuit simulations. These methods provides the fundamental evidences for the cause and effect relationship between the dynamics of the memristor couplings and the synchronization state types.

REFERENCES

[1] J. Rocabert, A. Luna, F. Blaabjerg and P. Rodriguez, "Control of Power Converters in AC Microgrids," *IEEE Trans. on Ind. Electron.*, vol. 27, no. 11, pp. 4734-4749, Nov. 2012.

[2] M. Li, B. Wei, J. Matas, J. M. Guerrero and J. C. Vasquez, "Advanced Synchronization Control for Inverters Parallel Operation in Microgrids Using Coupled Hopf Oscillators," *CPSS Trans. Power Electron Appl.*, vol. 5, no. 3, pp. 224-234, Sep. 2020.

[3] P. Maffezzoni, B. Bahr, Z. Zhang and L. Daniel, "Oscillator Array Models for Associative Memory and Pattern Recognition," *IEEE Trans. Circuits Syst. I Regul. Pap.*, no. 6, pp. 1591-1598, Jun. 2015.

[4] P. Maffezzoni, B. Bahr, Z. Zhang and L. Daniel, "Analysis and Design of Boolean Associative Memories Made of Resonant Oscillator Arrays," *IEEE Trans. Circuits Syst. I Regul. Pap.*, vol. 63, no. 11, pp. 1964-1973, Nov. 2016.

[5] M. R. Pufall, W. H. Rippard, G. Csaba, D. E. Nikonov, G. I. Bourianoff and W. Porod, "Physical Implementation of Coherently Coupled Oscillator Networks", *IEEE J. Explor. Solid-State Comput. Devices Circuits*, vol. 1, pp. 76-84, Aug. 2015.

[6] J. Liu, H. Li and J. Luo, "Impulse Bipartite Consensus Control for Coupled Harmonic Oscillators Under a Coopetitive Network Topology Using Only Position States", *IEEE Access*, vol 7, pp. 20316-20324, Feb. 2019.

[7] D. E. Nikonov, P. Kurahashi, J. S. Ayers, H. Li, T. Kamgaing, G. C. Dogiamis, H. J. Lee, Y. Fan and I. A. Young, "Convolution Inference via Synchronization of a Coupled CMOS Oscillator Array", *IEEE J. Explor. Solid-State Comput. Devices Circuits*, vol. 6, no. 2, pp. 170-176, Dec. 2020.

[8] L. Wetzel, D. Prousalis, R. F. Riaz, C. Hoyer, N. Joram, J. Fritzsche, F. Ellinger and F. Julicher, "Network Synchronization Revisited: Time Delays in Mutually Coupled Oscillators", *IEEE Access*, vol. 10, pp. 80027-80045, Aug. 2022.

[9] G. Yang, D. Tong, Q. Chen and W. Zhou,"Fixed-Time Synchronization and Energy Consumption for Kuramoto-Oscillator Networks With Multilayer Distributed Control", *IEEE Trans. Circuits Syst. II Regul. Pap*, vol. 70, no. 4, April 2023.

[10] L. O Chua, "Memristor-The Missing Circuit Element", *IEEE Trans. on Circuit Theory*, vol. CT-18, no. 5, pp. 507-519, Sep. 1971.

[11] D. B. Strukov, G. S. Snider, D. R. Stewart and R. S. Williams, "The missing memristor found", *Nature Lett.*, vol. 453, pp. 80-83, May 2008.

[12] Y. Setou, Y. Nishio and A. Ushida, "Synchronization Phenomena in Resistively Coupled Oscillators with Different Frequencies", *IEICE Trans. Fundam.*, vol. E79-A, no. 10, pp. 1575-1580, Oct. 1996.

[13] Y. Uwate and Y. Nishio, "Synchronization Phenomena in van der Pol Oscillators Coupled by Fifth-Power Nonlinear Resistor", *Proc. Int. Conf. NOLTA'07*, pp. 232-235, Sep. 2007.

[14] Y. Uwate, Y. Nishio and R. Stoop, "Complex Pattern in a Ring of van der Pol Oscillators Coupled by Time-Varying Resistors", *Int. J. Circuits, Syst. Comput.*, vol. 19, no. 4, pp. 819-834, Jun. 2010.

[15] J. Zhang and X. Liao, "Synchronization and chaos in coupled memristor-based FitzHugh-Nagumo circuits with memristor synapse," *Int. J. Electronics and Communications*, vol. 75, pp. 82-90, Mar. 2017.

[16] M. Itoh and L. O. Chua, "Memristor Oscillators", *Int. J. Bifurcation Chaos*, vol. 18, no. 11, pp. 3183-3206, Sep. 2008.